International Journal of Radiology and Diagnostic Imaging

E-ISSN: 2664-4444
P-ISSN: 2664-4436
Impact Factor (RJIF): 5.68
www.radiologypaper.com
IJRDI 2025; 8(3): 84-89
Received: 05-07-2025
Accepted: 07-07-2025

Dr. Nivedita Radder
Department of Radiology, University of Arkansas for Medical Sciences, Little Rock, Arkansas, USA

Dr. Shrinivas Radder
Department of Radiology, University of Arkansas for Medical Sciences, Little Rock, Arkansas, USA

Corresponding Author:
Dr. Nivedita Radder
Department of Radiology, University of Arkansas for Medical Sciences, Little Rock, Arkansas, USA

Critical patterns in metabolic brain imaging: A radiologist's guide to endogenous encephalopathies

Nivedita Radder and Shrinivas Radder

DOI: https://www.doi.org/10.33545/26644436.2025.v8.i3b.478

Abstract
Endogenous metabolic brain disorders represent a critical subset of neurological emergencies that require prompt recognition and management. This review examines the characteristic imaging patterns of five major endogenous metabolic encephalopathies: hypoxic-ischemic encephalopathy, posterior reversible encephalopathy syndrome (PRES), hepatic encephalopathy with hyperammonemia, hypoglycemic encephalopathy, and Wernicke encephalopathy. Understanding these distinct imaging patterns is essential for radiologists to facilitate rapid diagnosis and guide appropriate clinical management. We present a systematic approach based on anatomical distribution patterns and imaging characteristics, emphasizing the correlation between pathophysiology and radiological findings.

Keywords: Metabolic encephalopathy, magnetic resonance imaging, diffusion-weighted imaging, hypoxic-ischemic encephalopathy, posterior reversible encephalopathy syndrome, hepatic encephalopathy, hyperammonemia, uremic encephalopathy, hypoglycemic encephalopathy, wernicke encephalopathy, cytotoxic edema, vasogenic edema, pattern recognition, neuroimaging

Introduction
Metabolic brain disorders arise from disruptions in the delicate balance of metabolic substrates, neurotransmitters, electrolytes, and blood flow within the central nervous system (CNS) [1, 2]. While both exogenous toxins and endogenous metabolic derangements can affect the brain, this review focuses exclusively on endogenous causes that frequently present as acute encephalopathies in clinical practice. The brain's high metabolic demands and limited energy reserves make it particularly vulnerable to metabolic disturbances [3]. Imaging plays a pivotal role in the evaluation of these patients, who often present with altered mental status, seizures, or focal neurological deficits [4]. Recognition of characteristic imaging patterns can narrow the differential diagnosis and expedite appropriate treatment, potentially preventing irreversible neurological damage [5].

Pathophysiologic Basis of Imaging Findings
Understanding the pathophysiology of cerebral edema is fundamental to interpreting imaging findings in metabolic encephalopathies [6, 7]. Cytotoxic edema results from failure of cellular ion pumps due to energy depletion, leading to intracellular water accumulation. This manifests as restricted diffusion on diffusion-weighted imaging (DWI) with corresponding low apparent diffusion coefficient (ADC) values, with gray matter structures being preferentially affected [8]. In contrast, vasogenic edema is caused by blood-brain barrier disruption with leakage of fluid into the extracellular space. This appears as T2/FLAIR hyperintensity without diffusion restriction, predominantly affecting white matter [9].
Excitotoxic injury represents excessive glutamate release leading to neuronal injury. Certain brain regions with high densities of excitatory receptors, including the basal ganglia, thalami, cortical gray matter, periventricular white matter, and corpus callosum, show increased vulnerability to this mechanism of injury [3, 10]. This selective vulnerability explains many of the characteristic imaging patterns seen in metabolic encephalopathies.

Hypoxic-Ischemic Encephalopathy
Hypoxic-ischemic encephalopathy (HIE) results from global cerebral hypoperfusion or hypoxia, commonly following cardiac arrest, respiratory failure, or severe hypotension [11]. The severity and duration of the insult determine the extent and pattern of injury.^12^ HIE

demonstrates predictable patterns based on selective vulnerability of different brain regions [13]. In the acute phase (24-48 hours), mild-to-moderate injury manifests as bilateral symmetric involvement of watershed zones between major vascular territories [14] Severe injury results in extensive involvement of deep gray nuclei (putamen, caudate, thalami), cerebral cortex, and cerebellum [11]. The globus pallidus shows particular vulnerability due to its high metabolic demands [15].

MRI findings in HIE evolve over time. Initially, T2/FLAIR sequences may be normal or show only subtle hyperintensity. DWI demonstrates restricted diffusion in affected areas, reflecting cytotoxic edema (Figure 1). T1-weighted images may show loss of normal gray-white differentiation, and MR spectroscopy reveals elevated lactate peaks with reduced N-acetylaspartate [13, 16]. Prognostic indicators based on imaging include the extent and location of injury. Extensive cortical involvement suggests poor outcome, while isolated watershed injury indicates better prognosis. Bilateral thalamic and basal ganglia involvement correlates with poor neurological recovery [17].

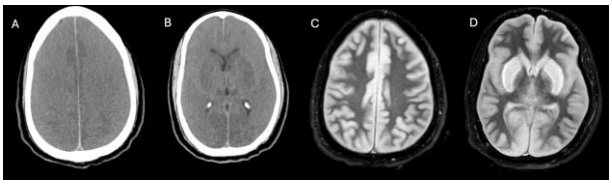

Fig 1: Hypoxic-ischemic encephalopathy imaging findings in the clinical setting of cardiac arrest. (A and B) Axial NECT demonstrates diffuse loss of gray-white matter differentiation with bilateral basal ganglia hypoattenuation, consistent with global hypoxic-ischemic injury. (C and D) Axial DWI sequences reveal extensive restricted diffusion involving both the cerebral cortex and deep gray matter structures, indicating acute cytotoxic edema characteristic of severe hypoxic-ischemic brain injury.

Posterior Reversible Encephalopathy Syndrome (PRES)

PRES represents a clinicoradiologic syndrome characterized by potentially reversible subcortical vasogenic brain edema [18]. Common precipitating factors include hypertensive crisis, preeclampsia/eclampsia, immunosuppressive therapy (particularly cyclosporine and tacrolimus), autoimmune disorders, and renal failure [19]. Current theories suggest endothelial dysfunction as the primary mechanism, whether from acute hypertension exceeding cerebral autoregulation or direct cytotoxic injury to endothelium [20].

The classic imaging distribution, seen in 90% of cases, involves bilateral parieto-occipital subcortical white matter, typically symmetric but occasionally asymmetric [21] (Figure 2). Other common patterns include the superior frontal sulcus pattern (70%) and watershed pattern (50%). MRI characteristics include T2/FLAIR hyperintensity in subcortical and deep white matter without restricted diffusion on DWI/ADC maps, consistent with vasogenic edema. However, areas of cytotoxic edema indicating infarction may be present. Enhancement is variable, seen in up to 37% of cases, and hemorrhage may complicate severe cases [22, 23].

Atypical patterns of PRES include the central variant affecting brainstem, basal ganglia, thalami, and periventricular white matter; the anterior variant with frontal lobe predominance; and rarely, unilateral involvement [24]. Most cases show complete resolution within 2-4 weeks with appropriate management of the underlying cause, though delayed treatment may result in permanent injury from cytotoxic edema and infarction [25].

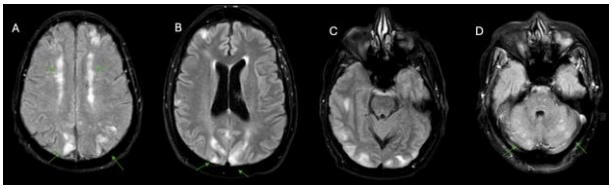

Fig 2: Posterior reversible encephalopathy syndrome (PRES) in the setting of renal failure. (A, B, C, D) Axial FLAIR MR images demonstrate bilateral symmetric cortical and subcortical hyperintensities involving both cerebral and cerebellar hemispheres, representing vasogenic edema typical of PRES. The distribution pattern shows the characteristic multifocal involvement beyond the classic parieto-occipital regions.

Hepatic Encephalopathy and Hyperammonemic Encephalopathy

Hepatic encephalopathy occurs in both acute fulminant hepatic failure and chronic liver disease with portosystemic shunting [26]. Hyperammonemic encephalopathy can also occur without liver disease in conditions such as urea cycle disorders, valproate toxicity, and parenteral nutrition [27]. The pathophysiology involves accumulation of neurotoxic substances, primarily ammonia and manganese, leading to astrocyte swelling from increased intracellular glutamine, alterations in neurotransmitter balance, and oxidative stress [28].

Chronic hepatic encephalopathy demonstrates characteristic bilateral T1 hyperintensity in the globus pallidi and substantiae nigrae in 80-90% of cases, attributed to manganese deposition [29, 30] (Figure 3). T2/FLAIR hyperintensity may be seen along corticospinal tracts, representing vasogenic edema. MR spectroscopy reveals elevated glutamine-glutamate peaks at 2.1-2.4 ppm with decreased myoinositol and choline, reflecting the brain's attempt to maintain osmotic balance [31].

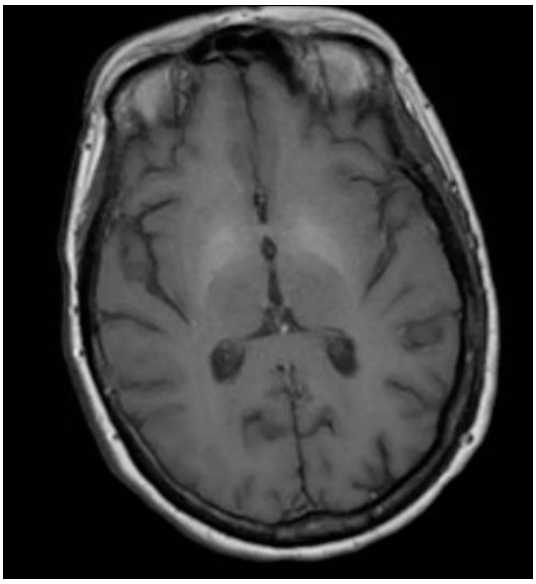

Fig 3: Chronic hepatic encephalopathy imaging findings. Axial T1-weighted image demonstrates characteristic bilateral symmetric T1 hyperintensity within the globus pallidi, a hallmark of manganese deposition secondary to impaired hepatic metabolism in chronic liver disease. This finding is pathognomonic for chronic hepatic dysfunction.

Acute hepatic and hyperammonemic encephalopathy demonstrate a different pattern, with bilateral involvement of insular and cingulate cortices showing relative sparing of perirolandic and occipital regions [27, 32] (Figure 4). Thalamic involvement is common and often shows restricted diffusion. DWI reveals strong restricted diffusion in affected cortical areas, and the severity of cortical involvement correlates with clinical outcomes, with extensive cortical involvement indicating more severe disease and poorer prognosis [33]. Imaging abnormalities may improve following treatment, though cortical involvement often indicates irreversible damage [34].

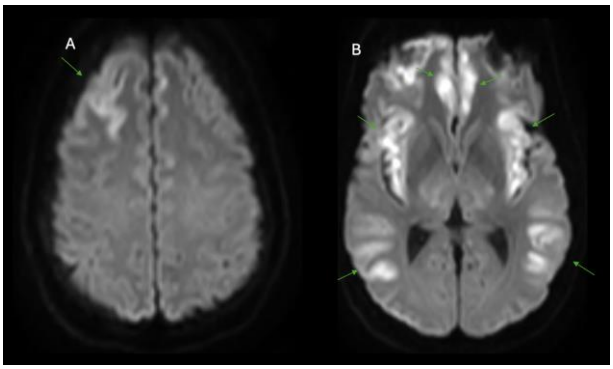

Fig 4: Acute hepatic encephalopathy with characteristic cortical involvement pattern. (A) Axial DWI demonstrates restricted diffusion in the right frontal cortex with notable sparing of the perirolandic region. (B) Bilateral symmetric diffusion restriction involving the insular and cingulate cortices along with temporal lobes, while characteristically sparing the occipital cortex. This distribution pattern of cytotoxic edema with perirolandic and occipital sparing is typical of acute hyperammonemic injury.

Uremic Encephalopathy

Uremic encephalopathy represents a distinct metabolic disorder occurring in the context of both acute and chronic renal failure, resulting from accumulation of uremic toxins including urea, creatinine, parathyroid hormone, and various organic acids [35]. The pathophysiology involves disruption of the blood-brain barrier, alterations in neurotransmitter metabolism, and direct neurotoxic effects of accumulated metabolites. Unlike other metabolic encephalopathies, uremic encephalopathy can present with a wide spectrum of neurological manifestations ranging from subtle cognitive impairment to severe encephalopathy with seizures.

Three main imaging patterns are recognized in uremic encephalopathy. The most common pattern involves the basal ganglia, particularly the lentiform nuclei, which show bilateral symmetric T2/FLAIR hyperintensity. The second pattern resembles PRES with cortical or subcortical involvement, likely related to concurrent hypertension and fluid overload commonly seen in renal failure. The third pattern involves predominantly white matter changes [35].

The lentiform fork sign (Figure 5) represents a characteristic but not pathognomonic finding in uremic encephalopathy. This sign is characterized by symmetric T2/FLAIR hyperintensity involving the basal ganglia and surrounding white matter structures, including the internal and external capsules and medullary laminae [36]. The hyperintense signal delineates the lateral and medial boundaries of both putamina, creating a distinctive fork-like appearance on axial images. This finding is more commonly observed in diabetic patients with uremia and is typically associated with concurrent metabolic acidosis. The presence of metabolic acidosis appears to be a critical factor in the development of this imaging pattern, suggesting that pH changes may contribute to the selective vulnerability of these structures.

DWI findings in uremic encephalopathy are variable, with some cases showing restricted diffusion indicating cytotoxic edema, while others demonstrate facilitated diffusion consistent with vasogenic edema. This variability likely reflects different stages and severities of the disease process. MR spectroscopy may reveal decreased N-acetylaspartate and increased choline peaks, reflecting neuronal dysfunction and membrane turnover.

The reversibility of imaging findings in uremic encephalopathy depends on the promptness of treatment. Early initiation of dialysis can lead to complete resolution of imaging abnormalities, particularly in cases showing predominantly vasogenic edema. However, areas of restricted diffusion may indicate irreversible injury. The lentiform fork sign, when present, often persists even after successful treatment, suggesting some degree of permanent structural change [36].

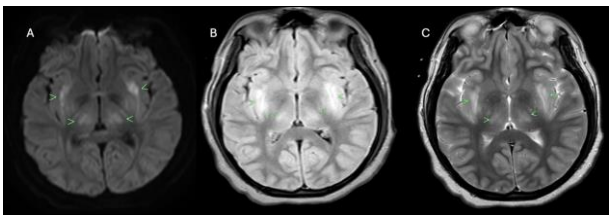

Fig 5: Uremic encephalopathy with characteristic lentiform fork sign. (A) Axial DWI, (B) Axial FLAIR, and (C) Axial T2-weighted images demonstrate bilateral symmetric signal abnormalities involving the lentiform nuclei and thalami. The hyperintense signal outlining the putamina creates the distinctive "lentiform fork sign," a characteristic finding in uremic encephalopathy typically associated with metabolic acidosis in renal failure.

Hypoglycemic Encephalopathy

Hypoglycemic brain injury occurs when blood glucose falls below critical levels, typically less than 2.2 mmol/L, most commonly in diabetic patients on insulin therapy, but also in cases of insulinoma, severe malnutrition, and neonates born to diabetic mothers [37]. The pathophysiology involves glucose deprivation leading to energy failure, particularly affecting regions with high metabolic demands and limited glycogen reserves [38].

The imaging pattern reflects selective vulnerability, with bilateral involvement of parieto-occipital and temporal cortices, hippocampi, and basal ganglia (the latter associated with poor outcome). A characteristic feature is sparing of the thalami, cerebellum, and brainstem, which helps distinguish hypoglycemic from hypoxic-ischemic injury [39, 40] (Figure 6). MRI findings include T2/FLAIR hyperintense signal in affected gray matter, restricted diffusion on DWI indicating cytotoxic edema, and early sulcal effacement from gyral swelling on T1-weighted images. The internal capsule and corona radiata may show symmetric involvement [41].

The neonatal pattern differs from that seen in adults, with posterior predominant injury affecting parieto-occipital gray and white matter, involvement of optic radiations, and posterior thalamic involvement [42]. This posterior predominance and thalamic sparing in adults helps

distinguish hypoglycemic from hypoxic-ischemic encephalopathy, which typically shows thalamic involvement and more diffuse distribution [39].

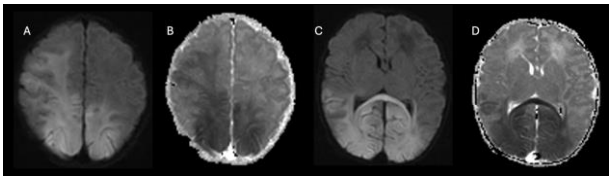

Fig 6: Hypoglycemic encephalopathy with characteristic posterior predominance. (A, B, C, D) Axial DWI and corresponding ADC maps demonstrate extensive cytotoxic edema with marked restricted diffusion predominantly affecting the parieto-occipital and temporal cortices bilaterally, with lesser involvement of the right frontal lobe. This posterior distribution pattern with relative sparing of the thalami, cerebellum, and brainstem is characteristic of hypoglycemic brain injury.

Wernicke Encephalopathy

Wernicke encephalopathy results from thiamine (vitamin B1) deficiency. While classically associated with chronic alcoholism, approximately 50% of cases occur in non-alcoholic conditions including hyperemesis (pregnancy-related or from chemotherapy), bariatric surgery, eating disorders, malabsorption syndromes, and prolonged parenteral nutrition [43, 44]. The classic clinical triad of confusion, ataxia, and ophthalmoplegia occurs in only 30% of patients, making imaging crucial for diagnosis [45].

Characteristic imaging locations include the medial thalami (85% of cases), mammillary bodies (60% of cases), periaqueductal gray matter (Figure 7) and tectal plate (66%), and hypothalamus. Less commonly involved sites include the dorsal medulla, cerebellum, and cranial nerve nuclei [46, 47]. MRI findings consist of symmetric T2/FLAIR hyperintensity in these characteristic locations, with possible restricted diffusion on DWI in the acute phase. Mammillary body enhancement is nearly pathognomonic and is seen in up to 80% of cases. Cortical involvement, when present, is occasionally asymmetric and typically affects the perirolandic regions [48].

Chronic changes include mammillary body atrophy and third ventricular enlargement [49]. Early treatment with thiamine can reverse imaging abnormalities and prevent progression to Korsakoff syndrome, emphasizing the importance of prompt recognition of this condition [50]. The combination of clinical suspicion and characteristic imaging findings, particularly symmetric involvement of the medial thalami and mammillary bodies with enhancement, should prompt immediate thiamine replacement even before laboratory confirmation.

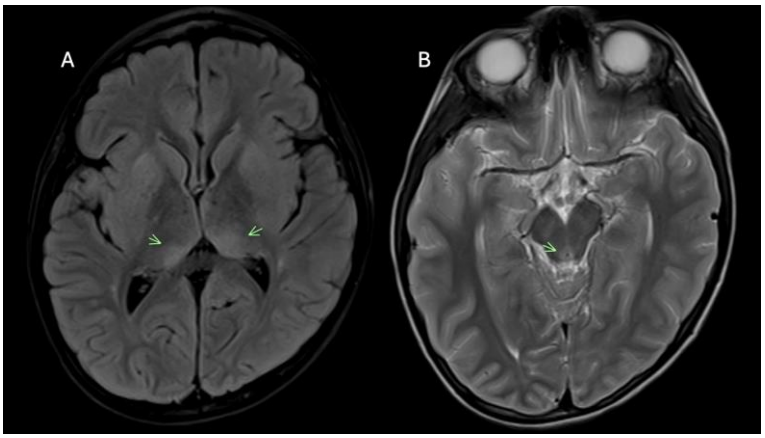

Fig 7: Wernicke encephalopathy demonstrating classic anatomical involvement. (A) Axial FLAIR image reveals bilateral symmetric hyperintensity within the medial thalami, a hallmark location for thiamine deficiency. (B) Axial T2-weighted image demonstrates a characteristic periaqueductal gray matter signal abnormality. The involvement of these symmetric midline structures, particularly the combination of medial thalamic and periaqueductal changes, is pathognomonic for Wernicke encephalopathy.

Differential Diagnosis and Pattern Recognition

A systematic pattern-based approach aids in the differential diagnosis of metabolic encephalopathies [2, 41]. Basal ganglia predominant patterns are seen in hypoxic-ischemic encephalopathy, hypoglycemic encephalopathy (with cortical involvement), chronic hepatic encephalopathy (characteristically T1 hyperintense), and uremic encephalopathy. Cortical predominant patterns include hypoglycemic encephalopathy with its characteristic parieto-occipital distribution, acute hyperammonemic encephalopathy affecting insular and cingulate cortices, and diffuse involvement in severe hypoxic-ischemic encephalopathy.

White matter predominant patterns are characteristic of PRES, with subcortical parieto-occipital involvement, and hepatic encephalopathy affecting the corticospinal tracts. Thalamic and mammillary body involvement strongly suggests Wernicke encephalopathy when the medial thalami and mammillary bodies are affected, though acute hepatic encephalopathy may also involve the thalami in conjunction with cortical changes. The presence of the lentiform fork sign suggests uremic encephalopathy, particularly when associated with known renal failure and metabolic acidosis.

Prognostic Implications

Understanding imaging patterns helps predict clinical outcomes in metabolic encephalopathies [17]. Favorable prognostic indicators include isolated white matter involvement, reversible vasogenic edema as seen in PRES, and early mammillary enhancement in Wernicke encephalopathy. These findings suggest potentially reversible injury with appropriate treatment. In contrast, poor prognostic signs include extensive cortical injury, bilateral basal ganglia involvement in HIE and hypoglycemia, and hemorrhagic transformation. The extent of restricted diffusion on DWI often correlates with the severity of irreversible injury, particularly in hypoxic-ischemic and hypoglycemic encephalopathies.

Conclusion

Recognition of characteristic imaging patterns in endogenous metabolic encephalopathies is essential for prompt diagnosis and management [2]. While overlap exists between different conditions, systematic evaluation of anatomical distribution, signal characteristics, and diffusion properties, combined with clinical context, enables accurate diagnosis in most cases. Early identification of these patterns can guide immediate therapeutic interventions, potentially preventing irreversible neurological damage and improving patient outcomes.

The radiologist plays a crucial role in recognizing these emergent conditions, particularly when clinical presentations are atypical or incomplete. The integration of clinical history, laboratory findings, and imaging patterns remains paramount for accurate diagnosis. Continued advancement in imaging techniques, including quantitative diffusion imaging and advanced MR spectroscopy, promises to further enhance our ability to diagnose and prognosticate these critical neurological conditions. As our understanding of the pathophysiology of these disorders evolves, so too will our ability to detect subtle imaging findings that may influence clinical management and ultimately improve patient outcomes.

Conflict of Interest

Not available.

Financial Support

Not available.

References

1. Osborn AG, Hedlund GL, Salzman KL. Toxic, metabolic, degenerative and CSF disorders. In: Osborn's Brain. 2nd ed. Philadelphia, Pa: Elsevier, 2017; 905-1155.
2. de Oliveira AM, Paulino MV, Vieira APF, *et al*. Imaging Patterns of Toxic and Metabolic Brain Disorders. RadioGraphics 2019;39:1672-1695.
3. Lipton SA, Rosenberg PA. Excitatory amino acids as a final common pathway for neurologic disorders. N Engl J Med 1994;330:613-622.
4. Valk J, van der Knaap MS. Toxic encephalopathy. AJNR Am J Neuroradiol 1992;13:747-760.
5. McKinney AM, Kieffer SA, Paylor RT, *et al*. Acute toxic leukoencephalopathy: potential for reversibility clinically and on MRI with diffusion-weighted and FLAIR imaging. AJR Am J Roentgenol 2009;193:192-206.
6. Schaefer PW, Buonanno FS, Gonzalez RG, Schwamm LH. Diffusion-weighted imaging discriminates between cytotoxic and vasogenic edema in a patient with eclampsia. Stroke 1997;28:1082-1085.
7. Na DG, Kim EY, Ryoo JW, *et al*. CT sign of brain swelling without concomitant parenchymal hypoattenuation: comparison with diffusion- and perfusion-weighted MR imaging. Radiology 2005;235:992-998.
8. Moritani T, Smoker WRK, Sato Y, *et al*. Diffusion-weighted imaging of acute excitotoxic brain injury. AJNR Am J Neuroradiol 2005;26:216-228.
9. Stokum JA, Gerzanich V, Simard JM. Molecular pathophysiology of cerebral edema. J Cereb Blood Flow Metab 2016;36:513-538.
10. Chokshi FH, Aygun N, Mullins ME. Imaging of acquired metabolic and toxic disorders of the basal ganglia. Semin Ultrasound CT MR 2014;35:75-84.
11. Huang BY, Castillo M. Hypoxic-ischemic brain injury: imaging findings from birth to adulthood. RadioGraphics 2008;28:417-439.
12. Chalela JA, Wolf RL, Maldjian JA, Kasner SE. MRI identification of early white matter injury in anoxic-ischemic encephalopathy. Neurology 2001;56:481-485.
13. Arbelaez A, Castillo M, Mukherji SK. Diffusion-weighted MR imaging of global cerebral anoxia. AJNR Am J Neuroradiol 1999;20:999-1007.
14. Howard RS, Holmes PA, Koutroumanidis MA. Hypoxic-ischaemic brain injury. Pract Neurol 2011;11:4-18.
15. Hegde AN, Mohan S, Lath N, Lim CC. Differential diagnosis for bilateral abnormalities of the basal ganglia and thalamus. RadioGraphics 2011;31:5-30.
16. Mlynash M, Campbell DM, Leproust EM, *et al*. Temporal and spatial profile of brain diffusion-weighted MRI after cardiac arrest. Stroke 2010;41:1665-1672.
17. Wijdicks EF, Campeau NG, Miller GM. MR imaging in comatose survivors of cardiac resuscitation. AJNR Am J Neuroradiol 2001;22:1561-1565.
18. Hinchey J, Chaves C, Appignani B, *et al*. A reversible posterior leukoencephalopathy syndrome. N Engl J Med 1996;334:494-500.
19. Bartynski WS. Posterior reversible encephalopathy syndrome, part 1: fundamental imaging and clinical features. AJNR Am J Neuroradiol 2008;29:1036-1042.
20. Bartynski WS. Posterior reversible encephalopathy syndrome, part 2: controversies surrounding pathophysiology of vasogenic edema. AJNR Am J Neuroradiol 2008;29:1043-1049.
21. McKinney AM, Short J, Truwit CL, *et al*. Posterior reversible encephalopathy syndrome: incidence of atypical regions of involvement and imaging findings. AJR Am J Roentgenol 2007;189:904-912.
22. Casey SO, Sampaio RC, Michel E, Truwit CL. Posterior reversible encephalopathy syndrome: utility of fluid-attenuated inversion recovery MR imaging in the detection of cortical and subcortical lesions. AJNR Am J Neuroradiol 2000;21:1199-1206.
23. Covarrubias DJ, Luetmer PH, Campeau NG. Posterior reversible encephalopathy syndrome: prognostic utility of quantitative diffusion-weighted MR images. AJNR Am J Neuroradiol 2002;23:1038-1048.
24. Gao B, Lyu C, Lerner A, McKinney AM. Controversy of posterior reversible encephalopathy syndrome: what have we learnt in the last 20 years? J Neurol Neurosurg Psychiatry 2018;89:14-20.
25. Rykken JB, McKinney AM. Posterior reversible encephalopathy syndrome. Semin Ultrasound CT MR 2014;35:118-135.
26. Ferenci P, Lockwood A, Mullen K, *et al*. Hepatic encephalopathy--definition, nomenclature, diagnosis, and quantification: final report of the working party at the 11th World Congresses of Gastroenterology, Vienna, 1998. Hepatology 2002;35:716-721.
27. U-King-Im JM, Yu E, Bartlett E, *et al*. Acute hyperammonemic encephalopathy in adults: imaging findings. AJNR Am J Neuroradiol 2011;32:413-418.
28. Häussinger D, Kircheis G, Fischer R, *et al*. Hepatic

encephalopathy in chronic liver disease: a clinical manifestation of astrocyte swelling and low-grade cerebral edema? J Hepatol 2000;32:1035-1038.
29. Rovira A, Alonso J, Córdoba J. MR imaging findings in hepatic encephalopathy. AJNR Am J Neuroradiol 2008;29:1612-1621.
30. Alonso J, Córdoba J, Rovira A. Brain magnetic resonance in hepatic encephalopathy. Semin Ultrasound CT MR 2014;35:136-152.
31. Grover VP, Dresner MA, Forton DM, *et al*. Current and future applications of magnetic resonance imaging and spectroscopy of the brain in hepatic encephalopathy. World J Gastroenterol 2006;12:2969-2978.
32. McKinney AM, Lohman BD, Sarikaya B, *et al*. Acute hepatic encephalopathy: diffusion-weighted and fluid-attenuated inversion recovery findings, and correlation with plasma ammonia level and clinical outcome. AJNR Am J Neuroradiol 2010;31:1471-1479.
33. Matsusue E, Kinoshita T, Ohama E, Ogawa T. Cerebral cortical and white matter lesions in chronic hepatic encephalopathy: MR-pathologic correlations. AJNR Am J Neuroradiol 2005;26:347-351.
34. Rosario M, McMahon K, Finelli PF. Diffusion-weighted imaging in acute hyperammonemic encephalopathy. Neurohospitalist 2013;3:125-130.
35. Kim DM, Lee IH, Song CJ. Uremic Encephalopathy: MR Imaging Findings and Clinical Correlation. AJNR Am J Neuroradiol 2016;37:1604-1609.
36. Kumar G, Goyal MK. Lentiform Fork sign: a unique MRI picture. Is metabolic acidosis responsible? Clin Neurol Neurosurg 2010;112:805-812.
37. Fujioka M, Okuchi K, Hiramatsu KI, *et al*. Specific changes in human brain after hypoglycemic injury. Stroke 1997;28:584-587.
38. Auer RN. Hypoglycemic brain damage. Forensic Sci Int 2004;146:105-110.
39. Kang EG, Jeon SJ, Choi SS, *et al*. Diffusion MR imaging of hypoglycemic encephalopathy. AJNR Am J Neuroradiol 2010;31:559-564.
40. Bathla G, Policeni B, Agarwal A. Neuroimaging in patients with abnormal blood glucose levels. AJNR Am J Neuroradiol 2014;35:833-840.
41. Sharma P, Eesa M, Scott JN. Toxic and acquired metabolic encephalopathies: MRI appearance. AJR Am J Roentgenol 2009;193:879-886.
42. Wong DS, Poskitt KJ, Chau V, *et al*. Brain injury patterns in hypoglycemia in neonatal encephalopathy. AJNR Am J Neuroradiol 2013;34:1456-1461.
43. Sechi G, Serra A. Wernicke's encephalopathy: new clinical settings and recent advances in diagnosis and management. Lancet Neurol 2007;6:442-455.
44. Santos Andrade C, Tavares Lucato L, da Graça Morais Martin M, *et al*. Non-alcoholic Wernicke's encephalopathy: broadening the clinicoradiological spectrum. Br J Radiol 2010;83:437-446.
45. Harper CG, Giles M, Finlay-Jones R. Clinical signs in the Wernicke-Korsakoff complex: a retrospective analysis of 131 cases diagnosed at necropsy. J Neurol Neurosurg Psychiatry 1986;49:341-345.
46. Zuccoli G, Gallucci M, Capellades J, *et al*. Wernicke encephalopathy: MR findings at clinical presentation in twenty-six alcoholic and nonalcoholic patients. AJNR Am J Neuroradiol 2007;28:1328-1331.
47. Manzo G, De Gennaro A, Cozzolino A, *et al*. MR imaging findings in alcoholic and nonalcoholic acute Wernicke's encephalopathy: a review. Biomed Res Int 2014;2014:503596.
48. Zuccoli G, Pipitone N. Neuroimaging findings in acute Wernicke's encephalopathy: review of the literature. AJR Am J Roentgenol 2009;192:501-508.
49. Sullivan EV, Pfefferbaum A. Neuroimaging of the Wernicke-Korsakoff syndrome. Alcohol Alcohol 2009;44:155-165.
50. Galvin R, Bråthen G, Ivashynka A, *et al*. EFNS guidelines for diagnosis, therapy and prevention of Wernicke encephalopathy. Eur J Neurol 2010;17:1408-1418.

How to Cite This Article
Dr. Abhay Shaileshbhai Patel, Dr. Athawale Tanmay Suneel, Dr. Jignesh Singh, Dr. Sudhanshu Chitravanshi. Functional outcome of posterior cruciate ligament substituted total knee arthroplasty. International Journal of Radiology and Diagnostic Imaging. 2025; 8(3): 84-89.